Far-field superlens for nanolithography*

Chen Jian(陈 健), Wang Qing-Kang(王庆康),† and Li Hai-Hua(李海华)

National Key Laboratory of Micro/Nano Fabrication Technology, Key Laboratory for Thin Film and Microfabrication Technology of Ministry of Education, Research Institute of Micro/Nano Science and Technology, Shanghai Jiao Tong University, Shanghai 200240, *China*

(Received 22 June 2009; revised manuscript received 30 July 2009)

A far-field optical lithography is developed in this paper. By designing the structure of a far-field optical superlens, lithographical resolution can be improved by using a conventional UV light source. The finite different time domain numerical studies indicate that the lithographic resolution at 50 nm line width is achievable with the structure shown in this paper by using 365 nm wavelength light, and the light can be transferred to a far distance in the photoresist.

Keywords: far-field, lithography, superlens, resolution

PACC: 4225B, 4230, 4230H, 7320J

1. Introduction

Since the invention of the integrated circuits, the patterns have been achieved by exposure technology. Photolithography has been a key technique in microfabrication over the past several years because of its high throughput, low cost, simplicity and reproducibility. However, due to the diffractive nature of the light, the resolution of conventional optical lithography is restricted by the wavelength of the illumination light. This is because far-field imaging systems can not retrieve evanescent waves which contain subwavelength details of an object but decays within the near field. According to the Abbe's theory, the resolution can be improved by using either shorter wavelengths or higher numerical apertures.[1] According to the current technology, combined with resolution enhancement technology, a 65 nm line width can be achieved by using the deep-UV light of 193 nm wavelength, and 45 nm or even 32 nm line width can be achieved with immersion lithography.[2] However, with the complicated surrounding system, the price and the operating cost of the equipment are very high.[3] How to break through the limit of the optical resolution is a great challenge and also of practical significance.

By collecting the evanescent waves, a near-field image with a resolution beyond the diffraction limit has recently been demonstrated.[4,5] Luo and Ishihara[6] have presented the surface plasmon resonant(SPR) interference nanolithography technique, used to fabricate fine patterns beyond the diffraction limit. But due to the nature of the exponential decay of evanescent waves, which carry the high spatial frequency imformation, 50-nm-wide lines are recorded in 50 nm of resist. It is near-field nanolithography. Pendry[7] predicted that a simple planar thin film termed a superlens could be used to produce optical imaging with a resolution below the diffraction limit. Pendry suggested that a lens having only one negative parameter would form an approximate superlens, and also suggested using silver due to its relatively low loss at a wavelength of 365 nm. The evanescent waves scattered from the object are coupled to collective electron oscillations on the metal surface, namely, the surface plasmon (SP), so the evanescent field is strongly enhanced by using the SPR.[8] And a single layer of metal can not transfer a subwavelength imaging to a far distance due to the material loss of the metal. In the present paper, we want to achieve line

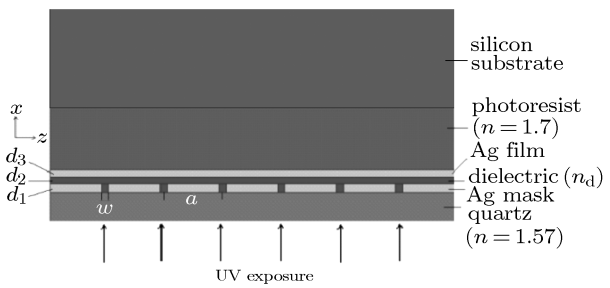


Fig. 1. Schematic drawing of FSL for lithography using a silver mask.

*Project supported by the Shanghai Committee of Science and Technology of China (Grant No. 0852nm06600) and the National Natural Science Foundation of China(Grant No. 60808014).

†Corresponding author. E-mail: wangqingkang@sjtu.edu.cn

© 2010 Chinese Physical Society and IOP Publishing Ltd

width $w = 50$ nm. According to the structure proposed in Refs. [9] and [10], we present the structure shown in Fig. 1, as a far-field superlens (FSL) for far field nanolithography.

2. Principle and numerical modeling

SPs are free electron density oscillations on the surface of metals in dielectric materials.[11] They exist only for the transverse magnetic (TM) wave polarization. The propagation of a surface plasmon is always coupled with a surface electromagnetic wave along the metal–dielectric boundary. In this paper, the surface plasmons excited on the metal mask (Ag) enhance the light through the subwavelength aperture. The surface plasmons conduce to confining the light intensity into the space behind the metal mask aperture by coupling.[12] The above mechanism is SPR, which is the resonance coupling between the incident light and the surface plasmon wave (SPW), and it can enhance the transmission. If the metal and the dielectric material are both semi-infinite, by solving Maxwell's equations from the boundary, the dispersion relation of SPs can be determined as[13]

$$k_{\rm sp} = k_0 \sqrt{\frac{\varepsilon_{\rm d}\varepsilon_{\rm m}}{\varepsilon_{\rm d} + \varepsilon_{\rm m}}}, \tag{1}$$

where $k_{\rm sp}$ is the wave vector of the surface plasmon; $\varepsilon_{\rm m}$ and $\varepsilon_{\rm d}$ are the permittivities of the metal and the dielectric material, and they must have opposite signs if SPs are possible to appear at such an interface. This condition is satisfied for metals because $\varepsilon_{\rm m}$ is both negative and complex. After calculation, $k_{\rm sp} > k_0$, which shows that SP leads to a near-field enhancement. In order to model the plasmonic response, the complex dielectric constant of metal at optical frequencies is approximated by the Drude model as follows:[14]

$$\varepsilon(\omega) = \varepsilon_\infty - \frac{\omega_{\rm p}^2}{\omega^2 + {\rm i}\,\gamma\omega}, \tag{2}$$

where ε_∞ is the infinite frequency permittivity, $\omega_{\rm p}$ is the plasma frequency, γ is the damping frequency, and $\omega = ck_0$ (c is the speed of light in vacuum) is the angular frequency of incident light. Here $\omega_{\rm p} = 1.3 \times 10^{16}$ rad/s, and $\gamma = 4.6 \times 10^{13}$ rad/s.[15] Silver film has permittivity $\varepsilon_{\rm m} = -2.5 + 0.69\,{\rm i}$ at a 365 nm wavelength. The evanescent field is strongly enhanced by surface plasmon resonance excitation on condition that $|\varepsilon_{\rm m}| \approx \varepsilon_{\rm d}$,[16] so the substrate should be of quartz (the refractive index $n = 1.57$). In order to reduce the reflection and the attenuation in the lossy metal, the total thickness of the structure must be much smaller than the wavelength.[17]

As shown in Fig. 1, $w = 50$ nm, $a = 400$ nm, the thicknesses of the Ag mask, dielectric, and sliver film are $d_1 = 20$ nm, $d_2 = 50$ nm, and $d_3 = 20$ nm, respectively. The thickness of the photoresist is 1 μm. In the FSL structure, the silicon will not affect the field distribution, but it could exert an influence on the field intensity because of its absorption and reflection. For simplicity, the silicon substrate is ignored in calculation. We must choose the refractive index of the dielectric ($n_{\rm d}$) so as to obtain high transmission efficiency and transfer the light to a far distance. To calculate the field distribution, a two-dimensional TM mode finite different time domain (FDTD) method is used. The boundary conditions along x and z directions are set to be of perfectly matched layer (PML) and periodical, respectively. In the 2D TM case, Maxwell's equations take the following form:

$$\frac{\partial H_y}{\partial t} = -\frac{1}{\mu_0}\left(\frac{\partial E_x}{\partial z} - \frac{\partial E_z}{\partial x}\right), \quad \frac{\partial E_x}{\partial t} = -\frac{1}{\varepsilon}\frac{\partial H_y}{\partial z}, \quad \frac{\partial E_z}{\partial t} = \frac{1}{\varepsilon}\frac{\partial H_y}{\partial x}. \tag{3}$$

The total set of numerical Eq. (3) takes the form[18]

$$H_y^n(i,k) = H_y^{n-1}(i,k) - \frac{\Delta t}{\mu_0 \Delta z}[E_x^{n-1/2}(i,k+1/2) - E_x^{n-1/2}(i,k-1/2)] + \frac{\Delta t}{\mu_0 \Delta x}[E_z^{n-1/2}(i+1/2,k) - E_z^{n-1/2}(i-1/2,k)], \tag{4a}$$

$$E_x^{n+1/2}(i,k+1/2) = E_x^{n-1/2}(i,k+1/2) - \frac{\Delta t}{\varepsilon \Delta z}[H_y^n(i,k+1) - H_y^n(i,k)], \tag{4b}$$

$$E_z^{n+1/2}(i+1/2,k) = E_z^{n-1/2}(i+1/2,k) + \frac{\Delta t}{\varepsilon \Delta x}[H_y^n(i+1,k) - H_y^n(i,k)], \tag{4c}$$

where the superscript n labels the time step while the indices i and k label the space steps and Δx and Δz along the x and the z directions, respectively. The time step is determined by the courant limit, i.e.

$$\Delta t \leq 1/(c\sqrt{1/(\Delta x)^2 + 1/(\Delta z)^2}). \tag{5}$$

3. Results and discussion

Figures 2(a), 2(b) and 2(c) show the distributions of magnetic field H_y of the designed FSL structure when $n_{\rm d} = 1.8$, 1.9 and 2, respectively. When $n_{\rm d} = 1.9$, the image quality is best. Using the FSL as presented in Fig. 1 leads to the enhancing of the evanescent waves and the transferring of a subwavelength imaging of 50 nm line width to the far distance. SPs are excited on both sides of the Ag mask. The incident light is scattered, owing to subwavelength features, into both propagating waves and evanescent waves. Because of the SPR, the evanescent waves have been enhanced on the surface of the Ag mask as shown in Fig. 3(a). And there are a few propagating waves through the slit. Through the dielectric, the evanescent waves are enhanced by the Ag film again, and they can transfer to a longer distance (about 300 nm).[19] Then the evanescent wave is strongly attenuated. According to the conservation of energy, the propagating wave field is strongly strengthened when the evanescent wave is strongly attenuated as shown in Fig. 3(b). So the propagating waves can propagate to the bottom of the 1 μm thick resist layer (Fig. 3(c)).

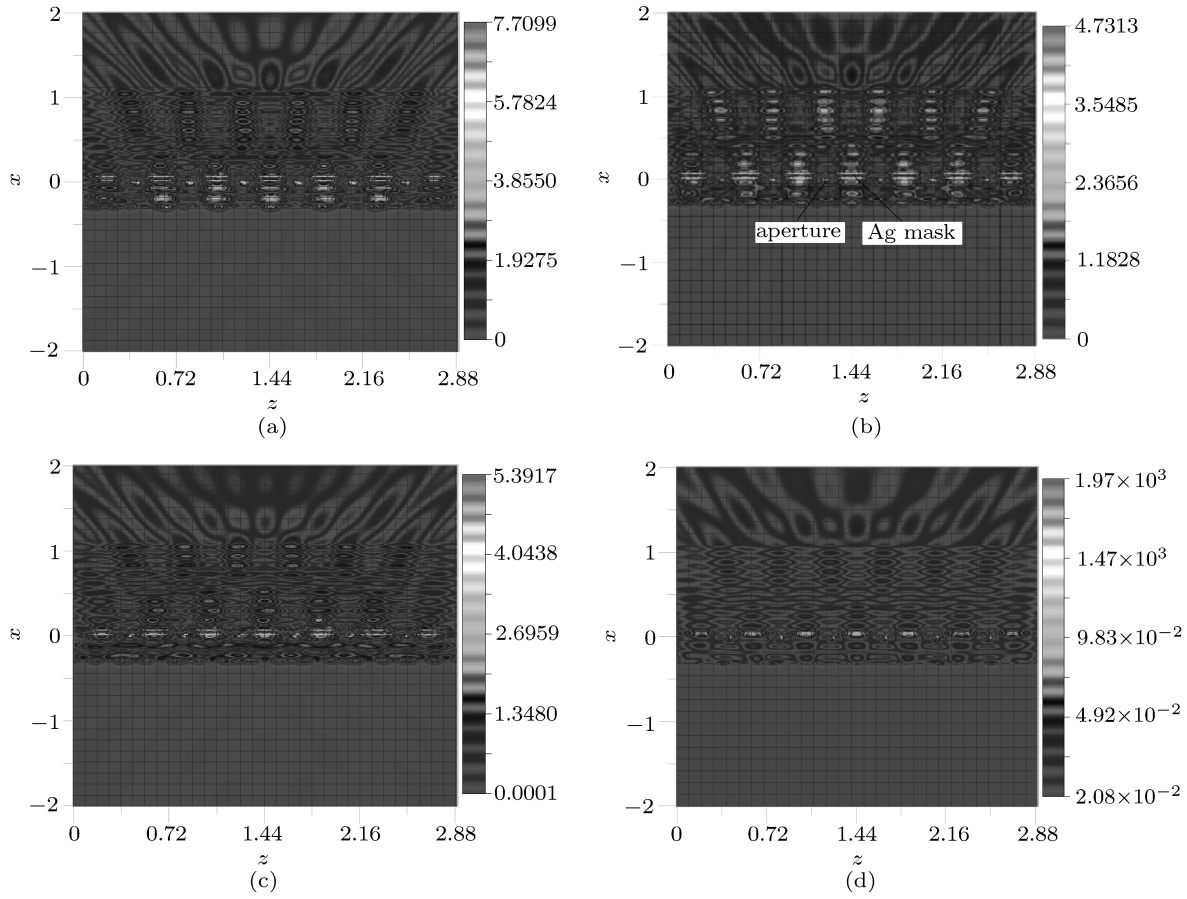


Fig. 2. Distributions of magnetic field H_y of the designed FSL structure with $n_{\rm d} = 1.8$ (a), $n_{\rm d} = 1.9$ (b), $n_{\rm d} = 2$ (c), and the distribution of electric-field E_z with $n_{\rm d} = 1.9$ (d).

Figure 2(d) shows the distribution of electric-field E_z with $n_{\rm d} = 1.9$. We can see that the field distribution is the same as that in Fig. 2(b), but the field intensity of E_z is more larger than that of H_y. By Eq. (4c) H_y and E_z are connected, which accords with Figs. 2(b) and 2(d). Here we need only the field distribution and the relative field intensity, so the magnetic field component H_y is basically shown in this paper.

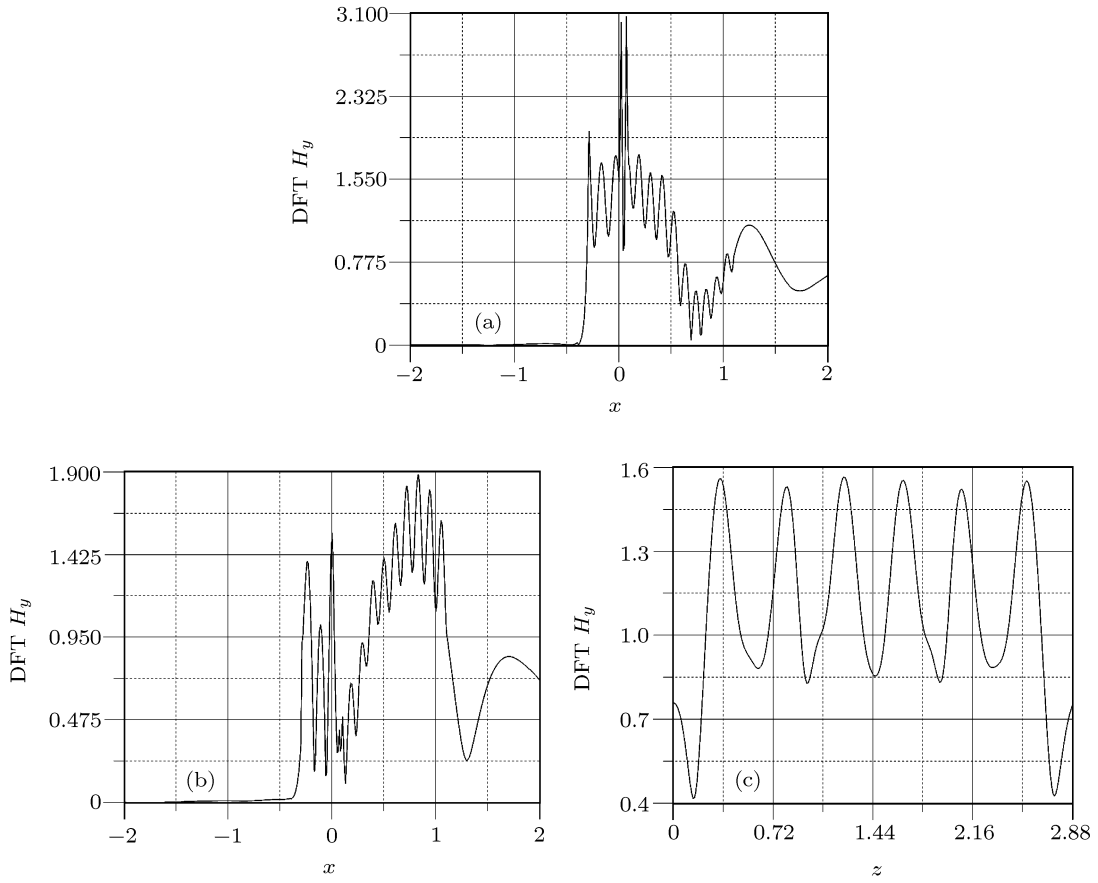


Fig. 3. (a) Longitudinal cross-section distribution of H_y by discretised Fourier transform (DFT) at the Ag mask ($z = 1.4$ μm); (b) longitudinal cross-section distribution of H_y at the pattern ($z = 1.2$ μm) (c) lateral cross-section distribution of H_y at a depth of 950 nm into the 1 μm thick resist layer ($x = 1.04$ μm);.

Figure 4 is the line scans of the intensity of H_y in front ($x = 20$ nm) and at the rear ($x = 70$ nm) of the dielectric ($n_{\rm d} = 1.9$). The intensity of H_y on the metal layer is enhanced by orders of magnitude due to the interaction of the SPs at the surfaces of the metal film with the incident light. On a smooth metal–dielectric interface, light does not couple to the surface plasmons because the conservations of energy and momentum are not obeyed. The grating momentum associated with the structure allows momentum conservation when the SPs interact with the incident light.[20]

When $d_2 = 40$ nm and 60 nm, the distributions of the magnetic field H_y are shown in Fig. 5. We can see that the role of the dielectric in the structure is to filter the light, so that only a little light can pass through the aperture and to separate it from the light on the surface of the Ag mask. When d_2 becomes smaller, it is not filtered enough as shown in Fig. 5(c). When d_2 becomes larger, it is filtered too enough to have lower energy as shown in Fig. 5(d). So we choose $d_2 = 50$ nm.

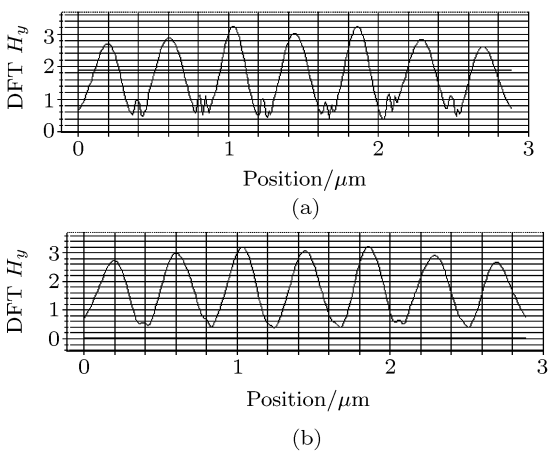


Fig. 4. Line scans of the intensity (lateral cross-section) of H_y with $n_{\rm d} = 1.9$ at $x = 20$ nm (a) and $x = 70$ nm (b).

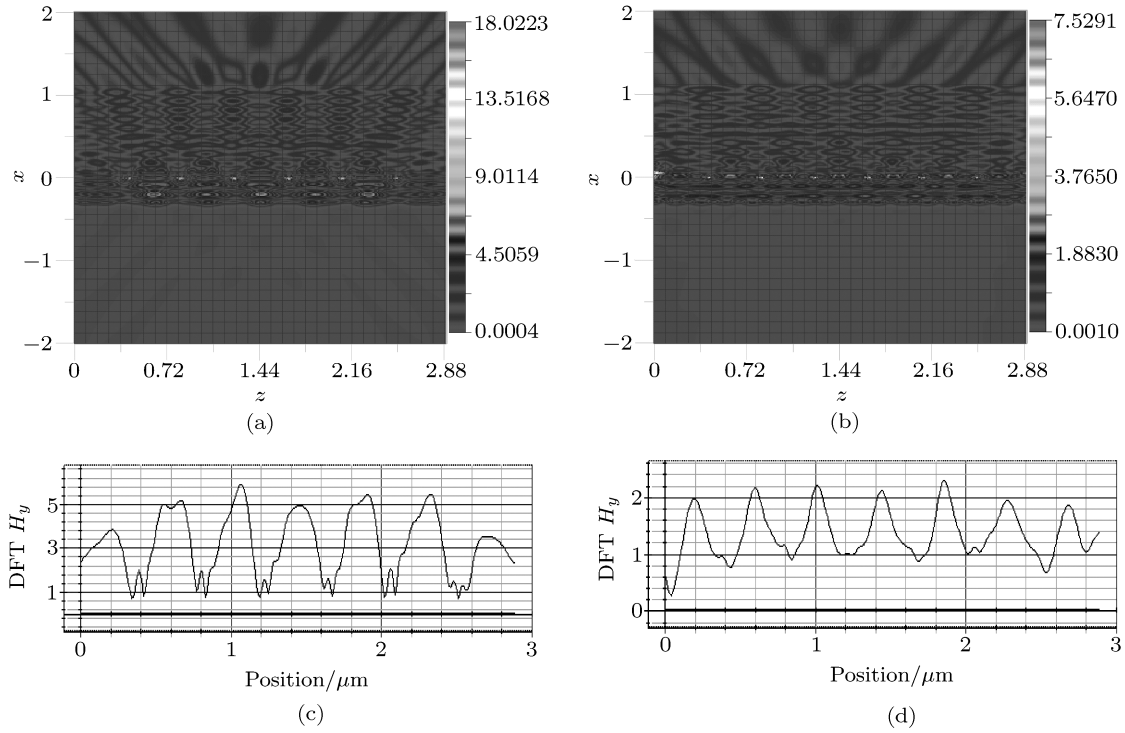


Fig. 5. Distributions of magnetic field H_y of the FSL structure with the same $n_{\rm d} = 1.9$, but with different values of d_2: (a) $d_2 = 40$ nm and (b) $d_2 = 60$ nm. The corresponding line scans of the intensity (lateral cross-section) of H_y at $x = 60$ nm (c) and $x = 80$ nm (d).

Without the Ag film, the distribution and the line scan of H_y are shown in Fig. 6. From Fig. 6(c) it follows that the role of the Ag slab is to focus the light into sharp imaging,[7,21] and because of the absorption and reflection of the Ag film the intensity of H_y is reduced.

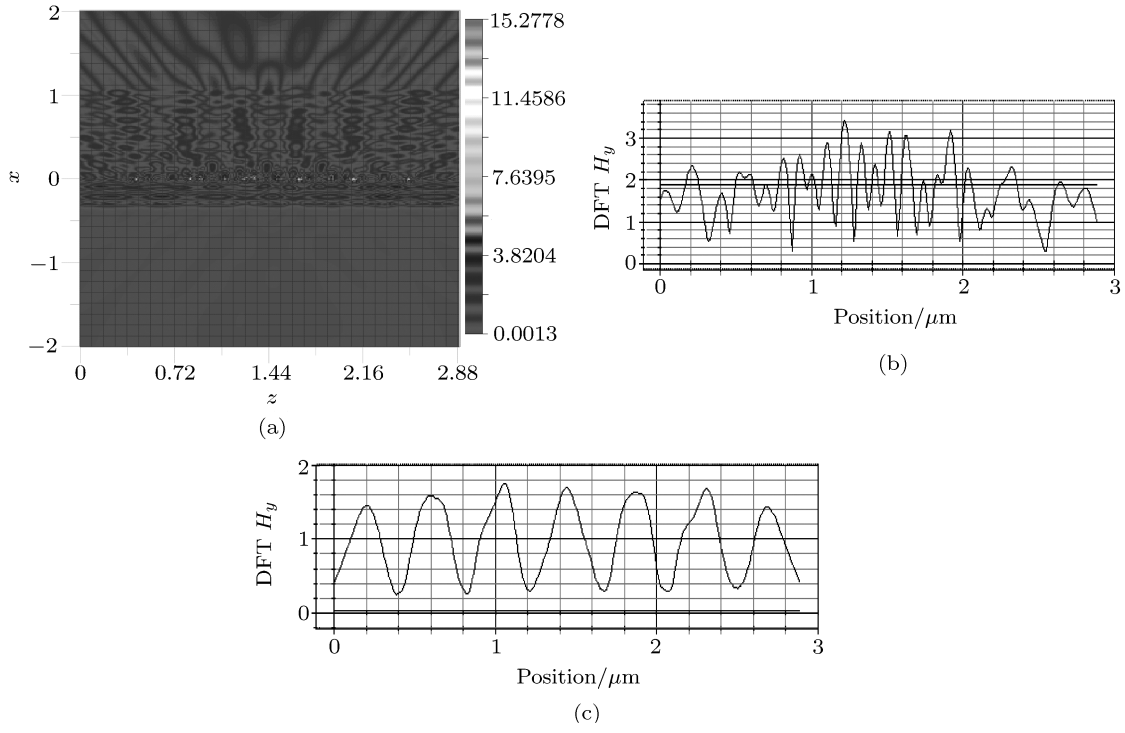


Fig. 6. (a) Distribution of magnetic field H_y of the designed structure with $n_{\rm d} = 1.9$ and $d_3 = 0$; (b) line scan of the intensity (lateral cross-section) of H_y at $x = 70$ nm with $n_{\rm d} = 1.9$ and $d_3 = 0$; (c) line scan of the intensity (lateral cross-section) of H_y at $x = 90$ nm with $n_{\rm d} = 1.9$ and $d_3 = 20$ nm.

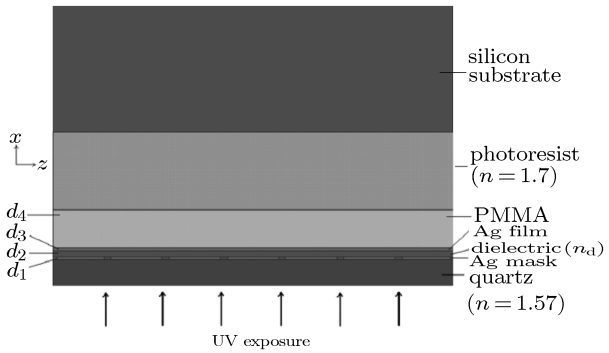


Fig. 7. New FSL structure with an additive PMMA layer.

In Fig. 2(b), propagating waves and evanescent waves are both in the photoresist, which is not useful for nanolithography. We should make the evanescent waves in another medium and only the propagating waves in the photoresist, so we improve the FSL structure, which is shown in Fig. 7. There is a polymethylmethacrylate (PMMA) ($n = 1.5$) layer between the photoresist and the Ag film, and its thickness is $d_4 = 300$ nm. The thickness of the photoresist is changed to 700 nm. The results are shown in Fig. 8. We can see that the H_y distribution is almost the same as that in Fig. 2(b), while the intensity of H_y is small compared with that in Fig. 2(c), which is because of the absorption and the reflection of the PMMA layer.

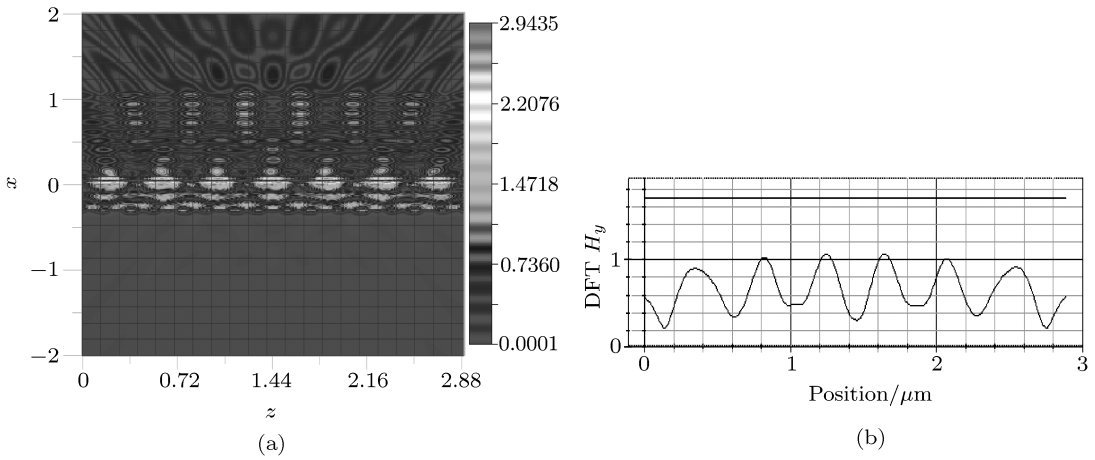


Fig. 8. (a) Distribution of magnetic field H_y of the FSL in Fig. 7 with $n_d = 1.9$, $d_1 = d_3 = 20$ nm, $d_2 = 50$ nm, and $d_4 = 300$ nm; (b) line scan of the intensity (lateral cross-section) of H_y at $x = 1.06$ μm, i.e. at a depth of 670 nm into the 700 μm thick resist layer.

Using the FSL structure as shown in Fig. 1, the line width smaller than 50 nm can also be achieved, and aperiodic patterns can also be obtained. This nanolithography technology is related to the distance between the patterns.

4. Conclusions

With the FSL structure presented in the paper, a higher lithographical resolution can be obtained by using a conventional UV light source. Also the subwavelength imaging can be transferred to a far distance. The FDTD simulations indicate that the transmissivity appears to be a function of periodicity and aperture size, as well as the medium.

References

[1] Levenson M D, Viswanathan N S and Simpson R A 1982 *IEEE Trans. Electr. Dev.* **29** 1828

[2] Hong X G, Xu W D, Li X G, Zhao C Q and Tang X D 2008 *Acta Phys. Sin.* **57** 6643 (in Chinese)

[3] Fang L, Du J L, Guo X W, Wang J Q, Zhang Z Y, Luo X G and Du C L 2008 *Chin. Phys.* B **17** 2499

[4] Melville D O S and Blaikie R J 2005 *Opt. Express* **13** 2127

[5] Fang N, Lee H, Sun C and Zhang X 2005 *Science* **308** 534

[6] Luo X G and Ishihara T 2004 *Appl. Phys. Lett.* **84** 4780

[7] Pendry J B 2000 *Phys. Rev. Lett.* **85** 3966

[8] Srituravanich W, Durant S, Lee H, Sun C and Zhang X 2005 *J. Vac. Sci. Technol.* B **23** 2636

[9] Liu Z, Durant S, Lee H, Pikus Y, Fang N, Xiong Y, Sun C and Zhang X 2007 *Nano Lett.* **7** 403

[10] Melville D O S and Blaikie R J 2007 *Physica* B **394** 197

[11] Guo J and Adato R 2008 *Opt. Express* **16** 1232

[12] Shao D B and Chen S C 2005 *Appl. Phys. Lett.* **86** 253107

[13] Barnes W L, Dereux A and Ebbesen T W 2003 *Nature* **424** 824

[14] Janssen O T A, Urbach H P and 't Hooft G W 2006 *Opt. Express* **14** 11823

[15] Quong M C and Elezzabi A Y 2007 *Opt. Express* **15** 10163

[16] Xiong Y, Liu Z, Durant S, Lee H, Sun C and Zhang X 2007 *Opt. Express* **15** 7095

[17] Li X, He S and Jin Y 2007 *Phys. Rev.* B **75** 045103

[18] Zhou Q, Zhu X and Li H F 2000 *Acta Phys. Sin.* **49** 210 (in Chinese)

[19] Hohng S C, Yoon Y C and Kim D S 2002 *Appl. Phys. Lett.* **81** 3239

[20] Thio T, Ghaemi H F, Wolff P A and Ebbesen T W 1999 *J. Opt. Soc. Am.* B **16** 1743

[21] Blaikie R J and Melville D O S 2005 *J. Opt.* A: *Pure Appl. Opt.* **7** 176